Experimental evaluation of the desuperheater influence in a CO_2 booster refrigeration facility

J. Catalán-Gil [a*], Daniel Sánchez [a], Ramón Cabello [a], Rodrigo Llopis [a], Laura Nebot-Andrés [a], Daniel Calleja-Anta [a]

[a]Jaume I University, Dep. of Mechanical Engineering and Construction, Campus de Riu Sec s/n E-12071, Castellón, Spain

*Corresponding author: jcatalan@uji.es Tel.: +34 964 728133; Fax.: +34 964 728106

ABSTRACT

Commercial refrigeration has undergone significant changes in recent years. In the European market, this is mainly due to the F-Gas Regulation (EU 517/2014). F-Gas affects in great measure to commercial centralized refrigeration systems for supermarkets with cooling load higher than 40kW, where the use of refrigerants with GWP higher than 150 will be banned in 2022. As a long-term solution, CO_2 has been adopted as unique refrigerant in almost all Europe overcoming the main technology hurdles. The use of booster systems in supermarkets allow covering simultaneously the medium and the low temperature services with different cycle configurations depending on the environmental conditions. The use of the desuperheater between both compression stages is a simple method to reduce the temperature at the suction port of the medium-temperature compressors improving its efficiency and therefore reducing its power consumption. The benefits of using this arrangement in terms of power consumption, discharge temperature, optimum pressure and COP, are experimentally evaluated and discussed in this work with increments in COP up to 7.05 %.

KEYWORDS

Commercial refrigeration, CO_2, Booster, experimental evaluation, desuperheater

HIGHLIGHTS

- A fully monitored CO2 transcritical booster facility is presented.
- The effect of desuperheater (DSH) is experimentally tested and discussed.
- DSH reduces the discharge temperature of the medium-temperature compressor (MTc) up to 10K.
- DSH increases the global efficiency of the MTc up to 8.45%.
- DSH increases the COP of the facility up to 7.05%.

Nomenclature

Abbreviations

BP	back pressure valve
COP	coefficient of performance
DSH	desuperheater
GC/K	gas cooler/condenser
GWP	global warming potential
h	specific enthalpy ($kJ \cdot kg^{-1}$)
LT	low temperature
LR	load ratio
$\dot{m}$	mass flow rate ($kg \cdot s^{-1}$)
MT	medium temperature
P	pressure (bar)
PAG	polyalkylene glycol
$\dot{Q}$	thermal capacity (W)
T	temperature (°C)
USH	useful superheat
$\dot{V}_g$	compressor swept volume ($m^3 \cdot s^{-1}$)
$\dot{V}$	volumetric flow rate ($m^3 \cdot h^{-1}$)
v	volume ($m^3 \cdot kg^{-1}$)
$\dot{W}_{elec}$	power consumption (W)

Greek Symbols

Δ	variation (increment or decrement)
ε	relative error (%) / thermal effectiveness
η_G	global efficiency
η_V	volumetric efficiency
ρ	density ($kg \cdot m^{-3}$)

Subscripts

C	compressor
CO_2	carbon dioxide
EV	expansion valve
GC	gas-cooler
g	mixture water and glycol
in	inlet / in
K	condenser
N	compressor speed (rpm)
O	evaporator
out	out / outlet
ref	refrigerant
suc	suction
T	temperature (°C)
vol	volumetric
w	water

1 Introduction

The European regulation F-Gas [1], which gets into force in 2015, affects significantly to commercial centralized refrigeration systems in the commercial sector. At Annex III.13 of F-Gas are established new limits for the refrigerants used in this type of systems for cooling load higher than 40kW. For these facilities it is necessary to use refrigerants with GWP_{100} lower than 150 in the primary circuit (direct expansion systems) and lower than 1500 for secondary circuits (indirect expansion systems or cascade arrangements).

At present, there are several A1 refrigerants with GWP lower than 1500 that can be used in indirect systems as R134a (GWP_{100}=1.300) or its drop-ins R513A (GWP_{100}=573) and R450A (GWP_{100}=547), but taking into account the quotas established at F-Gas or Kigali's amendment to Montreal Protocol [2] for placing HFCs on the market, the trend is being to use natural refrigerants for centralized refrigeration systems. Among all of natural refrigerants, CO_2 is one of the most used solution in recent years due to different characteristics such as high volumetric capacity, lower cost than other refrigerants, very low GWP (GWP_{100}=1) or high safety level (A1 class), among others. However, the lower efficiency of CO_2 systems at high environmental temperatures (transcritical operation), makes the basic refrigeration system not as efficient as other refrigerants for warm-hot climates [3,4].

For this reason, in climates with high environmental temperature, systems with CO_2 has been traditionally used in subcritical conditions as low-temperature fluid in cascade systems [5] or as secondary fluid in indirect systems [6]. However, the regulation of refrigerants with high GWP100 in primary circuits promote the use of CO_2 booster architectures as an interesting solution for covering to low and medium temperature services in commercial refrigeration applications. The main advantage of these systems is the use of a unique fluid classified as A1 security with no charge limitations instead of others fluids with low-GWP100 such as R152a, R717 or pure HFOs, among others.

CO2 booster systems are designed to work in both transcritical and subcritical conditions and its efficient performance fully depends on the environmental temperatures and the configuration adopted in the refrigeration facility. In warm or hot climates where transcritical operation is commonly reached, the basic configuration of CO_2 boosters needs some modifications to improve its energy efficiency resulting in more complex and costly cycles than the basic system [7].

Among the different existing solutions to improve the efficiency of the CO_2 booster systems, one of these with low complexity is to introduce a heat exchanger after the low temperature compressors rack (LT_C) denoted desuperheater (DSH). This heat exchanger denoted as desuperheater (DSH) has been experimentally analysed by Cavallini et al. [8] in a CO_2 compound system with a unique service at low-temperature, and by Llopis et al. [9] in the low-temperature cycle of a cascade system also with a unique service at low-temperature. However, to the best of authors knowledge there is not experimental analysis performed in CO_2 booster architectures, where the benefits of cooling down the refrigerant before entering the medium temperature compressors could be relevant due to the high energy consumption of these.

Another basic improvement is the use the flash-gas by-pass valve with the aim of reducing the accumulator tank pressure and the vapour quality at the inlet of evaporators. The use of this configuration allows decreasing the mass flow rate in evaporators and also reducing the temperature at the injection point. This arrangement has been experimentally tested by Cabello et al. [10] in a single-stage CO_2 transcritical vapour compression cycle and by Elbel & Hrnjak et al. [11] in a transcritical CO_2 system with a double-stage compression.

Finally, the most extended solution is the use of an internal heat exchanger (IHX) located before the low temperature expansion valve to cool down the refrigerant with the aid of the cool vapour from the low-temperature evaporator. This heat exchanger has been theoretically and experimentally analysed by Cavallini et al. [8] in a two-stage transcritical CO_2 cycle, and by Rigola et al. [12] and Torrella et al. [13] in a single-stage transcritical CO_2 cycle.

Other advanced CO_2 transcritical systems include the use of parallel compression [14] [15] to reduce the power consumption of the MT_C, the use of flooded evaporators [16] increasing the evaporation level, the heat recovery to heat tap water, space heating and air conditioning [17], the use of mechanical subcooling systems [18], or the use of ejectors as jet-pump increasing the evaporative level of evaporators and improving the expansion process [19,20]. Additionally, there are other less studied methods that improve the efficiency of transcritical systems, such as the one studied by Aprea et al. [21], in which a desiccant wheel is analysed to increase energetic performance in a CO_2 transcritical cycle.

Taking into account the basic solutions existing for CO_2 booster systems, this work is addressed to analyse experimentally the energy impact of installing a desuperheater heat exchanger in an own designed and mounted CO_2 Booster architecture with IHX, which solution has not been analysed experimentally in detail in the literature for CO_2 Booster architecture operating at two different evaporating temperatures. Experimental tests have been performed at three heat rejection temperatures: 15, 25 and 34 ºC in order to covering a wide range of environmental temperatures in warm climates. For each temperature, the rejection pressure was tested from the minimum possible to about 100 bar keeping constant the cooling load at the low and medium temperature evaporators: 0.9 kW and 2.7 kW, respectively. Finally, global COP, power consumption of the refrigerating plant, optimum pressure and suction/discharge temperature of the medium temperature compressor have been obtained and compared.

2 Experimental plant

To perform the experimental test that allows comparing the impact of installing the desuperheater in a CO_2 Booster with two different evaporating levels, an experimental facility has been developed (Fig. 1). This facility has been designed to test several improvements for CO_2 Booster such as flash gas (FG), parallel compression (PC), dedicated mechanical subcooling (DMS) and integrated mechanical subcooling (IMS) but they are not analysed in this work because the purpose is to analyse a basic improvement for booster system with low economic cost. This facility has many elements to ensure the proper operation. The cooling load and heat sink is provided by three independent loops, two of them using water/glycol mixture.

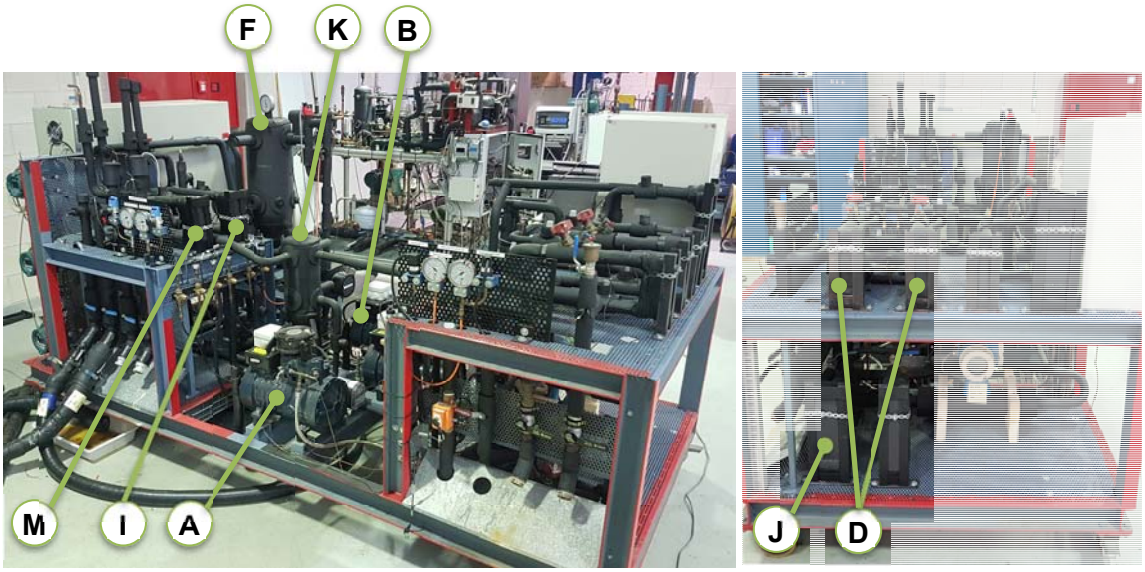

Fig. 1. CO_2 Booster plant.

The configurations analysed in this work are schematized in Fig. 2, which is composed with two semi-hermetic reciprocating compressors, one dedicated to MT level (B in Fig. 2) and the other one to LT (A in Fig. 2). The subcritical one (LT_C), has a displacement of 1.12 m^3/h at 1450 rpm (50Hz). However, the transcritical one (MT_C) has a displacement of 1.46 m^3/h (50Hz) and incorporates a fan on the head in order to reduce the high discharge temperatures. Both compressors are controlled by a variable frequency driver (VFD) and use PAG68 lubricant oil. After each compressor there is a coalescent oil separator (C in Fig. 2) to return oil to compressors.

The facility incorporates three electronic expansion valves, one to expand the refrigerant to LT_o, another to expand the refrigerant to MT_o (L and H in Fig. 2) and another one used as back-pressure valve that controls the rejection pressure of the facility (E in Fig. 2).

Since the use of the IHX is a well-known method to enhance the COP of transcritical cycles [12], the facility incorporates a tube-in-tube IHX (G in Fig. 2) with counter current layout and heat transfer area of 0.05 m^2. This heat exchanger cools down the saturated liquid from the accumulator receiver (F in Fig. 2) with the cold vapour from the low-temperature evaporator (T in Fig. 2). The effect of the IHX reduces the temperature at the inlet of the expansion valve (H in Fig. 2) and increases the temperature at the suction port of LT_C (B in Fig. 2), providing a higher temperature to the lubricant oil [22].

The others heat exchangers (HX) used in the facility are brazed-plate HX with the following heat transfer areas: 1.16 m^2 for GC/K (D in Fig. 2), 0.46 m^2 for MT_O and LT_O (M and I in Fig. 2) and 0.17 m^2 for the DSH (J in Fig. 2). To avoid heat transfer with the surroundings, the heat exchangers and all pipes have been isolated with an insulated material (thickness from 10 to 16 mm).

The operation with booster facilities requires three different temperature levels: the heat rejection drain, the MT_O level (around -6 °C) and the LT_O stage (around -32 °C). The first one is provided by an external water-loop that allows controlling temperature and volumetric flow. The last two are controlled by two external glycol loops where a mixture of water/propylene-glycol (70/30% in volume) is used for the medium temperature and a mixture of water/ethylene-glycol (60/40% in volume) is used for the low temperature level. Is important to notice that the desuperheater (J) is fed with the same temperature level used in the gas-cooler (D in Fig. 2).

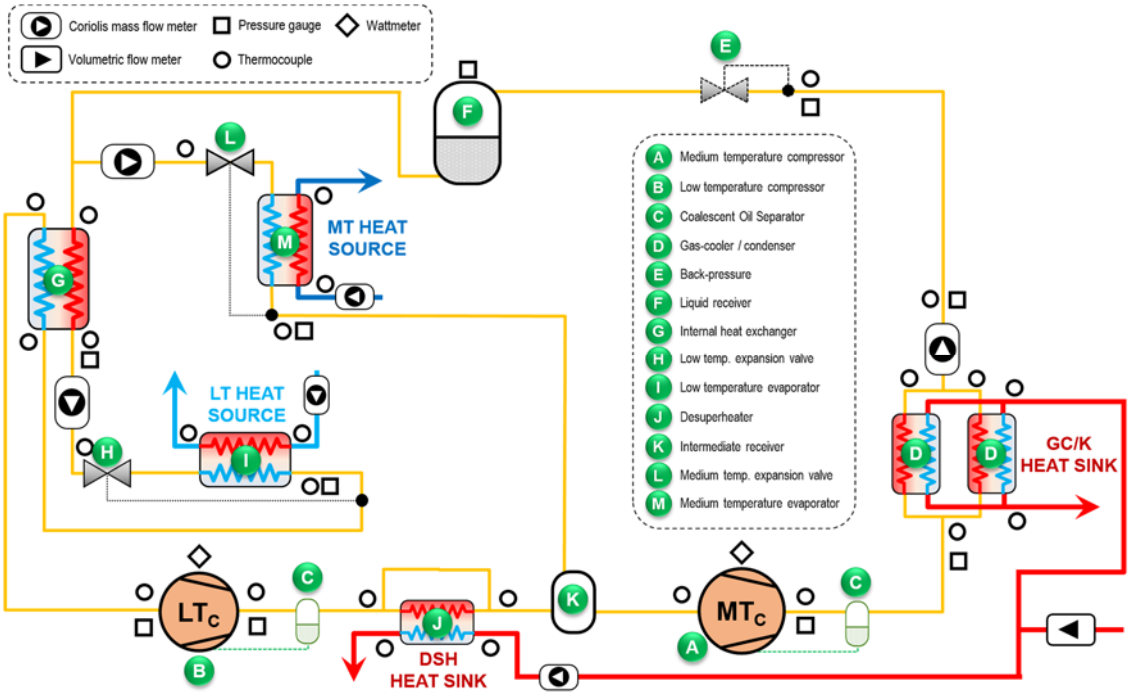

Fig. 2. Scheme of the refrigeration system and the sensor placement.

For the experimental analysis of the refrigerating plant, a complete data acquisition system has been installed including 27 T-type thermocouples with an accuracy, 2 pressure gauges (0 – 60 bar), 4 pressure gauges (0-100 bar) and 4 pressure gauges (0-160 bar). Moreover, the system includes two digital wattmeters to measure the power consumption of compressors, 3 Coriolis mass flow meters installed in the refrigerant loop, 2 Coriolis mass flow meters installed in the glycol loops, 1 Coriolis mass flow meters installed in the water loop of the desuperheater, and finally 1 magnetic flow meter installed in the water loop of the GC/K.

All data are gathered by a cRIO data acquisition system and handled with a developed application based on LabView®. The energy parameters uncertainties have been calculated as detailed by Moffat [23]. These data of the sensors and measurement devices used in the booster facility are summarized in Table 1 and the uncertainty of indirect measurements in Table 2.

Table 1. Calibration range and accuracy of the measurement devices.

Measured device	Sensors	Measured variable	Calibration range	Calibrated accuracy
T-type thermocouple	27	Temperature	-40 ÷ 145 °C	± 0.5 °C
Pressure gauge 0-160	4	Pressure	0 ÷ 60 bar	± 0.3 bar
Pressure gauge 0-100	4	Pressure	0 ÷100 bar	± 0.5 bar
Pressure gauge 0-60	2	Pressure	0 ÷ 160 bar	± 0.8 bar
Coriolis flow meter 1	1	GC/K refrigerant mass flow	0 ÷ 0.03 kg s^{-1}	± 0.23% of reading
Coriolis flow meter 2	1	MTo refrigerant mass flow	0 ÷ 0.02 kg s^{-1}	± 0.23% of reading
Coriolis flow meter 3	1	LTo refrigerant mass flow	0 ÷ 0.01 kg s^{-1}	± 0.23% of reading
Coriolis flow meter 4	1	LT volumetric flow (glycol)	0 ÷ 0.2 m^3 h^{-1}	± 0.5% of reading
Coriolis flow meter 5	1	MT volumetric flow (glycol)	0 ÷ 1 m^3 h^{-1}	± 0.5% of reading
Coriolis flow meter 6	1	DSH volumetric flow (water)	0 ÷ 0.1 m^3 h^{-1}	± 0.85% of reading
Magnetic flow meter	1	Heat sink volumetric flow (water)	0 ÷ 0.5 m^3 h^{-1}	± 0.5% of reading
Digital wattmeter	2	Power consumption	0 ÷ 4 kW	± 0.5% of reading
Analog signal (Inverter drive)	2	Compressor speed	0 ÷ 2030 rpm	± 1% of reading

Table 2. Uncertainty of the indirect measurements.

Parameter	Unit	Accuracy
COP	-	±2% to ±4.5%
Q LT_O (CO_2)	(kW)	±1.9% to ±3.1%
Q MT_O (CO_2)	(kW)	±1.3% to ±4.9%
Q GC/K (CO_2)	(kW)	±1.2% to ±2.7%
Q IHX (CO_2)	(kW)	±8.9% to ±16.1%
ηv MTC	-	±7.2% to ±10.1%
ηg MTC	-	±7.3% to ±9.8%

3 Refrigeration configurations analysed

The refrigeration system presented in Fig. 2 can operate with two different configurations: basic booster (BB) and basic booster with desuperheater (BB+DSH).

3.1 Basic booster (BB)

The BB configuration operates with two compressors. The LT_C compress the refrigerant from the low to the medium temperature evaporation level while the MT_C compress the refrigerant from the medium temperature level to the heat rejection pressure. Accordingly, the GC/K can operate in subcritical (below ≈74 bar) or transcritical conditions (above ≈74 bar). When it works in transcritical the rejection pressure is kept to a certain level using the BP, controlling the rejection pressure in order to operate at optimum working conditions [24].

Downstream the BP it is placed a liquid receiver where the CO_2 is in saturated conditions. Part of this refrigerant is expanded (MT_{EV}) to medium evaporation temperature and the rest is expanded (LT_{EV}) to the low-temperature level. Moreover, an internal heat exchanger (IHX) is

added before the LT_{EV} to increase the refrigerant temperature in LT_C suction line and to subcool the CO_2 before entering the LT_{EV}.

3.2 Basic booster with desuperheater (BB+DSH)

This configuration consists in the same architecture previously described but with another heat exchanger named desuperheater (DSH) located between the LTC discharge and the MTC suction (J in Fig. 2).

This heat exchanger is not generally considered in CO_2 boosters due to its additional cost, however it reduces the temperature from about 90ºC (common LT_C discharge temperature) to the heat rejection conditions temperature.

4 Experimental method

The systems stated before has been tested at three water rejection temperatures (15ºC, 25ºC and 34ºC), corresponding to the sending temperatures of the rig used as heat sink (GC/K temperature inlet in water rig). The two evaporation levels depend on the compressors displacement but these levels are near to -6ºC at medium temperature evaporator (MT_O) and near to -32ºC at low temperature evaporator (LT_O) with a superheating degree around 5.5K in the two evaporators. In order to keep a cooling load ratio (LR) between MT and LT evaporators around 3 that is commonly used in supermarkets [25–27], the cooling capacity at both evaporators has been kept constant: 2.7 kW for the MT_O and 0.9 kW for the LT_O.

For each rejection temperature, the pressure of the gas-cooler/condenser was varied from 65 to 110 bar to identify the optimum pressure that maximizes COP according to Kauf [28] and Chen and Gu [29], among other authors. This procedure has been repeated for the BB and BB+DSH configurations. In total, 41 steady-state tests of 20 min for each booster configuration have been done. The test had 2 seconds of sampling rate.

Regarding the DSH, in this work a water current has been used as secondary fluid to reject the heat from the discharge line of the LT_C. However, in commercial refrigeration plants, this heat dissipation is carried out by a finned-tube heat exchanger with an air fan. The power consumed by this fan affects the global COP of the facility as is stated in Equation (1), so for its calculation an additional consumption of 40 W ($P_{DSH,fan}$) has been considered when the DSH is used.

$$COP = \frac{\dot{Q}_{LTo} + \dot{Q}_{MTo}}{P_{LTc} + P_{MTc} + P_{DSH,fan}} \quad (1)$$

Table 3 summarizes the experimental test range evaluation and the variation of the main energy parameters of the plant. The data corresponding to the dark coloured headers are the values that were kept constants in all steady-state tests.

Table 3. Experimental test range.

SYSTEM	REJECTION TEMP. TEST (°C)	Gas-cooler / condenser						Desuperheater					COP
		$T_{water,in}$ (°C)	$\dot{V}_{water}$ ($m^3\ h^{-1}$)	$T_{ref,out}$ (min/max) (°C)	$\dot{m}_{ref}$ (min/max) ($kg\ s^{-1}$)	P_{ref} (min/max) (bar)	$\dot{Q}_{ref}$ (min/max) (W)	$T_{water,in}$ (°C)	$\dot{V}_{water}$ ($m^3\ h^{-1}$)	$T_{ref,out}$ (min/max) (°C)	$\dot{m}_{ref}$ (min/max) ($kg\ s^{-1}$)	$\dot{Q}_{ref}$ (min/max) (W)	
BB	15	15.00 ± 0.03	0.240 ± 0.001	15.1 ÷ 20.0	0.0169 ÷ 0.0185	65.4 ÷ 90.1	4559 ÷ 4731	-	-	-	-	-	1.987
	25	25.10 ± 0.03	0.240 ± 0.001	25.1 ÷ 28.2	0.0190 ÷ 0.0208	78.6 ÷ 95.1	4991 ÷ 5095	-	-	-	-	-	1.346
	34	34.00 ± 0.05	0.240 ± 0.001	34.3 ÷ 36.1	0.0218 ÷ 0.0237	91.3 ÷ 100.1	5515 ÷ 5603	-	-	-	-	-	0.995
BB+DSH	15	15.00 ± 0.03	0.240 ± 0.001	15.0 ÷ 19.9	0.0169 ÷ 0.0185	65.4 ÷ 90.1	4463 ÷ 4662	15.2 ± 0.05	0.050 ± 0.001	16.40 ÷ 16.56	0.0040 ÷ 0.0043	181 ÷ 203	2.045
	25	25.10 ± 0.03	0.240 ± 0.001	25.1 ÷ 28.0	0.0190 ÷ 0.0208	78.5 ÷ 95.1	4855 ÷ 4953	25.1 ± 0.04	0.050 ± 0.001	25.7 ÷ 25.77	0.0044 ÷ 0.0047	192 ÷ 218	1.404
	34	34.00 ± 0.13	0.240 ± 0.002	34.3 ÷ 36.1	0.0219 ÷ 0.0236	91.3 ÷ 100.1	5288 ÷ 5485	33.9 ± 0.11	0.050 ± 0.001	33.8 ÷ 33.94	0.0049 ÷ 0.0053	185 ÷ 223	1.065

		Low temperature evaporator						Medium temperature evaporator					
		$T_{glycol,in}$ (°C)	$\dot{V}_{glycol}$ ($m^3\ h^{-1}$)	T_O (°C)	$\dot{m}_{ref}$ (min/max) ($kg\ s^{-1}$)	USH (K)	$\dot{Q}_{ref}$ (W)	$T_{glycol,in}$ (°C)	$\dot{V}_{glycol}$ ($m^3\ h^{-1}$)	T_O (°C)	$\dot{m}_{ref}$ (min/max) ($kg\ s^{-1}$)	USH (K)	$\dot{Q}_{ref}$ (W)
BB	15	-20.00 ± 0.01	0.110 ± 0.002	-30.6 ± 0.1	0.0040 ÷ 0.0043	6.0 ± 0.5	897 ± 2	4.00 ± 0.05	0.400 ± 0.002	-5.4 ± 0.1	0.0130 ÷ 0.0143	5.3 ± 0.1	2702 ± 2
	25	-20.00 ± 0.04	0.110 ± 0.002	-32.2 ± 0.4	0.0044 ÷ 0.0047	5.1 ± 0.3	900 ± 2	4.00 ± 0.02	0.400 ± 0.003	-6.1 ± 0.1	0.0147 ÷ 0.0162	5.5 ± 0.1	2702 ± 7
	34	-20.00 ± 0.11	0.110 ± 0.002	-31.1 ± 0.3	0.0049 ÷ 0.0054	5.6 ± 0.3	898 ± 5	4.00 ± 0.03	0.400 ± 0.002	-5.8 ± 0.5	0.0170 ÷ 0.0184	5.4 ± 0.1	2699 ± 4
BB+DSH	15	-20.00 ± 0.06	0.110 ± 0.002	-30.1 ± 0.2	0.0040 ÷ 0.0043	5.5 ± 0.2	897 ± 2	4.00 ± 0.06	0.400 ± 0.003	-5.4 ± 0.1	0.0130 ÷ 0.0143	5.3 ± 0.1	2700 ± 1
	25	-20.00 ± 0.01	0.110 ± 0.001	-31.6 ± 0.2	0.0044 ÷ 0.0047	5.7 ± 0.4	898 ± 2	4.00 ± 0.05	0.400 ± 0.006	-5.9 ± 0.1	0.0147 ÷ 0.0161	5.5 ± 0.1	2701 ± 3
	34	-20.00 ± 0.08	0.110 ± 0.002	-30.9 ± 0.3	0.0049 ÷ 0.0053	5.3 ± 0.2	898 ± 4	4.10 ± 0.02	0.400 ± 0.002	-5.9 ± 0.3	0.0170 ÷ 0.0183	5.5 ± 0.1	2700 ± 3

To validate the acquired data, the heat transfer rate has been calculated at both sides of all brazed-plate heat exchangers: refrigerant and secondary fluid. To consider that mass flow rates, pressures and temperatures are measured correctly, the comparison between both heat transfer values must be negligible.

At the GC/K, the heat transferred in the refrigerant and the secondary fluid (water) is calculated with the Equation (2) and the Equation (3) for water side. This last, was determined using the volumetric flow rate through the GC/K, which is obtained from the total flow of water minus the flow through the desuperheater.

$$\dot{Q}_{GC/K,ref} = \dot{m}_{ref} \cdot \left[\frac{\left(h_{GC/K1,in} - h_{GC/K1,out}\right) + \left(h_{GC/K2,in} - h_{GC/K2,out}\right)}{2}\right] \quad (2)$$

$$\dot{Q}_{GC/K,water} = (\dot{V}_{w,total} \cdot \rho_{w,GC/K} - \dot{m}_{w,DSH}) \cdot \overline{C_{p,w,GC/K}} \cdot \left(T_{w,GC/K,out} - T_{w,GC/K,in}\right) \quad (3)$$

At the DSH, the heat from the refrigerant is calculated with Equation (4). The heat from water is determined with the Equation (5) for water side.

$$\dot{Q}_{DSH,ref} = \dot{m}_{ref} \cdot \left(h_{DSH,in} - h_{DSH,out}\right) \quad (4)$$

$$\dot{Q}_{DSH,water} = \dot{V}_{w,DSH} \cdot \rho_{w,DSH} \cdot \overline{C_{p,w,DSH}} \cdot \left(T_{w,GC/K,out} - T_{w,GC/K,in}\right) \quad (5)$$

In the low temperature evaporator, the cooling load provided by the refrigerant (Equation (6)) was contrasted with the heat from the water-ethylene glycol mixture (Equation (7)).

$$\dot{Q}_{LTo,ref} = \dot{m}_{LTo,ref} \cdot \left(h_{LTo,out} - h_{LTo,in}\right) \quad (6)$$

$$\dot{Q}_{LTo,glycol} = \dot{V}_{LTo,g} \cdot \rho_{w,LTo} \cdot \overline{C_{p,g,LTo}} \cdot \left(T_{g,in} - T_{g,out}\right) \quad (7)$$

For the medium temperature evaporator, the cooling load of the refrigerant is calculated with Equation (8) and compared with that provided by the water-propylene glycol mixture Equation (9).

$$\dot{Q}_{MTo,ref} = \dot{m}_{MTo,ref} \cdot \left(h_{MTo,out} - h_{MTo,in}\right) \quad (8)$$

$$\dot{Q}_{MTo,glycol} = \dot{V}_{MTo,g} \cdot \rho_{w,MTo} \cdot \overline{C_{p,g,MTo}} \cdot \left(T_{g,in} - T_{g,out}\right) \quad (9)$$

The software Refprop v9.1. [30] was used to evaluate the thermophysical properties of CO2, while SecCool Properties v1.33 [31] was used to calculate the properties for water and glycol mixtures. In all Equations stated before, isenthalpic process was assumed in all expansion valves. The results of Equation (2) to (9) are depicted in Fig. 3 and Fig. 4.

In addition, the global and volumetric efficiencies of the compressors have been calculated using Equations (10) and (11).

$$\eta_{global} = \dot{m}_{ref\_Comp.} \cdot \frac{\left(h_{iso_{out\ Comp.}} - h_{in\ Comp.}\right)}{P_{C,Comp.}} \quad (10)$$

$$\eta_{vol} = \frac{\dot{m}_{ref\_Comp.} \cdot v_{suc\_Comp.}}{\dot{V}_{G\_Comp.}} \quad (11)$$

Fig. 3 shows the heat balance in the low temperature evaporator between the refrigerant and the glycol side with differences below 7% with a constant cooling load in the refrigerant near of 0.9kW. Moreover, the heat balance differences in the DSH between the refrigerant and water side are below 10% with a heat transfer in DSH from 0.185kW to 0.225kW.

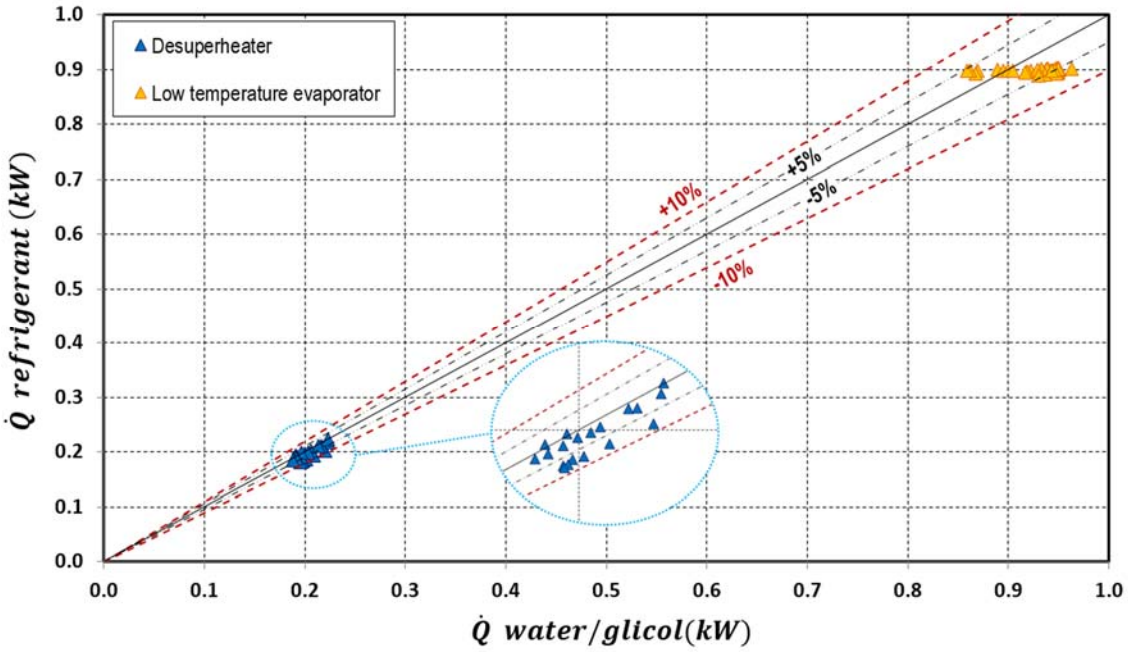

Fig. 3. Heat transfer validation in the low-temperature evaporator (LT_O) and desuperheater (DSH).

Fig. 4 shows the heat balance of the medium temperature evaporator with a cooling load near of 2.7kW. The maximum difference between refrigerant and the water-glycol is below 5%. Moreover, maximum difference between the refrigerant and water in the GC/K is also kept below 5% with a heat transfer from 4.4kW to 5.45kW.

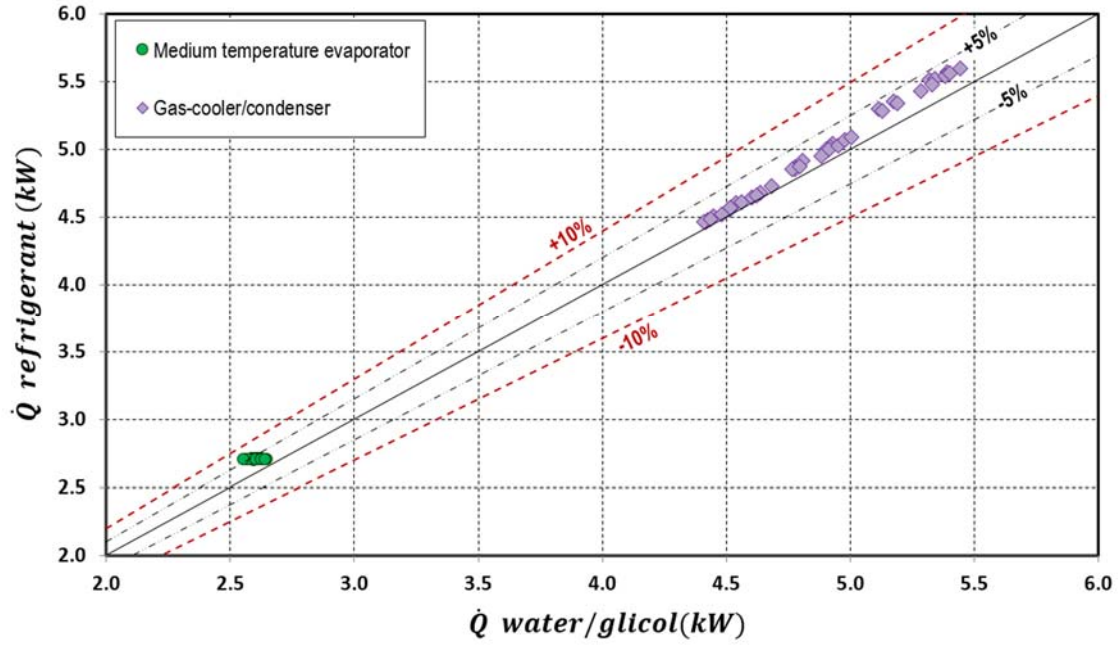

Fig. 4. Heat transfer validation in the medium-temperature evaporator (MT_O) and in the gas-cooler/condenser (GC/K).

In summary, the differences of the heat transfer rates between CO_2 and secondary fluids cases are always below 10% and the vast majority below 5%. Hence, the measures from experimental test can be assumed as correct and the heat losses to the environment can be assumed as negligible due to the good agreement of the heat balance in the heat exchangers.

5 Results and discussion

This section is devoted to present and discuss the experimental results obtained with the CO_2 Booster configurations tested. The first part of section 5 analyses the main differences in the P-h diagram when the DSH is added in the refrigerating plant. The second part focuses on analysing the performance of compressors including discharge and suction temperatures, volumetric and global efficiency and power consumption. Finally, the last part analyse the effect over the global COP of the refrigerating plant.

5.1 P-h diagrams

Fig. 5 shows in a P-h diagram, the main differences between the BB and BB+DSH configurations. The depicted cycles have been obtained at steady-state conditions operating at the maximum COP point for a rejection temperature of 34ºC.

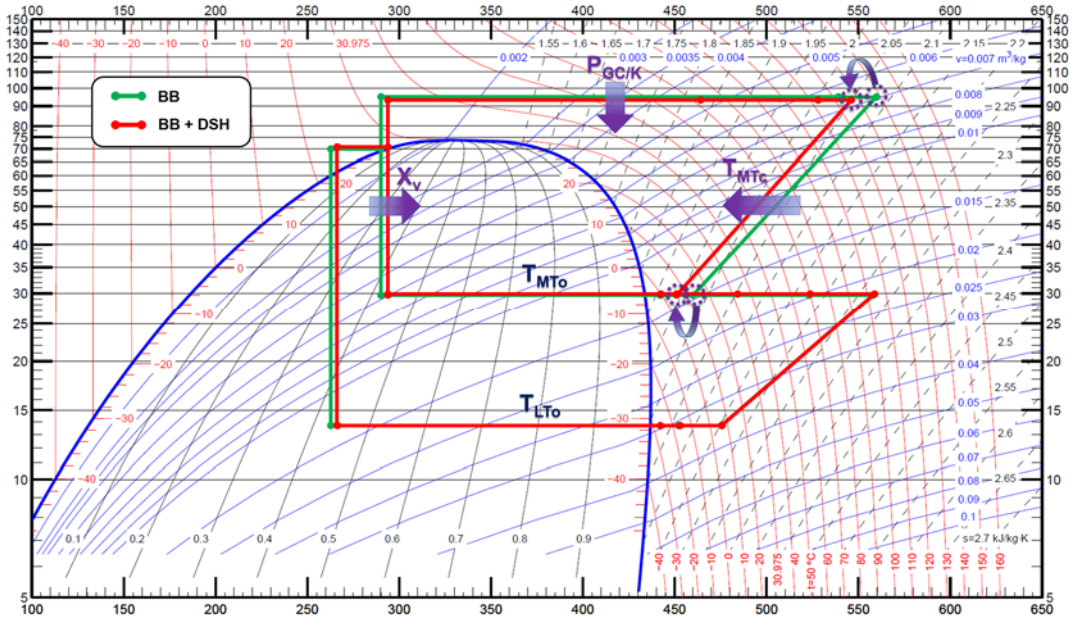

Fig. 5. P-h diagram of BB and BB+DSH.

From Fig. 5, three remarkable differences can be observed when the desuperheater is installed. The first one is the reduction of temperature in the suction port and the discharge line of the MT_C. This effect benefits the compressor global efficiency which affects its power consumption.

The second one is the reduction of the optimum pressure which also improves the compressor power consumption due to the reduction of the pressure ratio. However, this reduction increases the liquid receiver pressure as well as the vapour quality at the inlet of both evaporators (the third one difference). For this reason, if the cooling load is kept constant in both evaporators, the mass flow rate through them will be slightly greater when the desuperheating is installed.

5.2 Medium temperature compressor performance

As shown in the Fig. 5, the use of the desuperheater mainly affects the suction and the discharge line of the medium temperature compressor. Because of this, this section is focused on analysing this compressor including suction and discharge temperatures, global and volumetric efficiency and electrical power consumption.

5.2.1 Suction and discharge temperatures

The nature of carbon dioxide results always in high discharge temperature levels especially operating with high-pressure ratios or with a high superheating degree at suction port. High discharge temperatures are not desirable due to the oil degradation so the use of the DSH helps to reduce the discharge temperature.

Fig. 6 presents the temperature values measured at the suction port and the discharge line for the two configurations analysed.

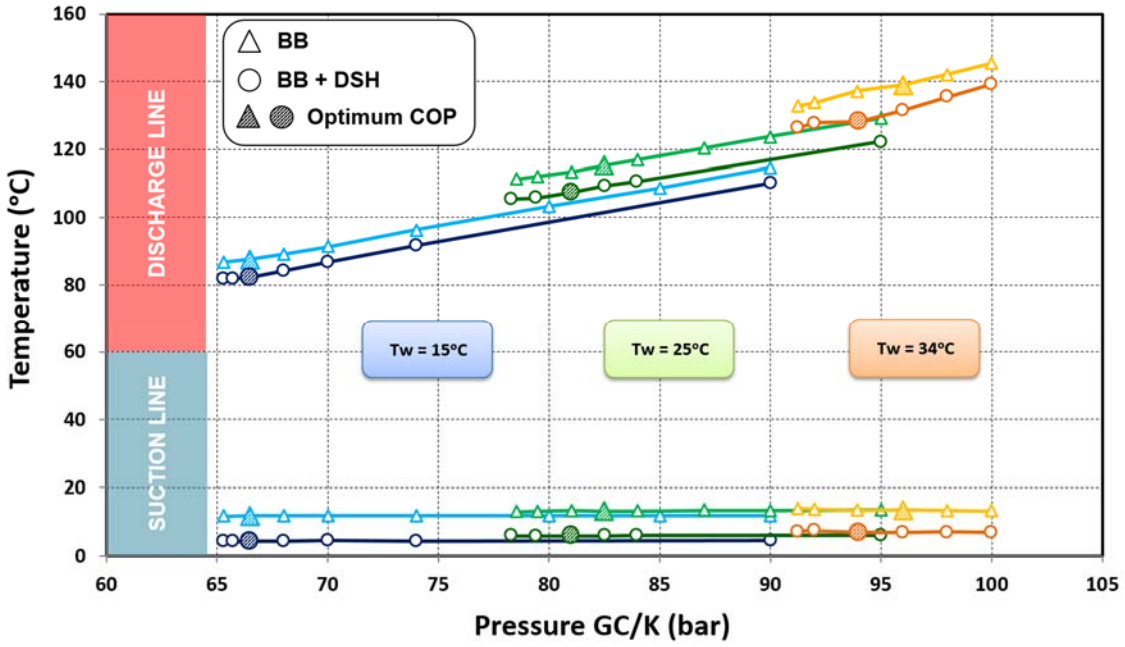

Fig. 6. MTc suction/discharge temperatures.

Fig. 6 incorporates the data obtained at the heat rejection temperature of 15ºC, which data are presented in blue from 65-90 bar, 25ºC, which data correspond to green lines from 78 to 95 bar, and 34ºC, that are depicted with orange lines from 91-100 bar.

Comparing the basic booster configuration (BB) respect to the basic booster with desuperheater (BB+DSH), the BB+DSH always provides a temperature reduction in the suction of the MT_C and consequently, in the discharge temperature, which, rises linearly with the GC/K pressure. Moreover, the temperature reduction in the suction line of the system using the DSH is quite similar at the three rejection temperatures analysed (about 7K). However, the reduction at the discharge temperature is not equal in all cases and it becomes higher as higher the heat rejection temperature is. From the experimental values, there is a reduction of 5K at the heat rejection temperature of 15ºC, 7K at 25ºC and up to 10K at 34ºC.

5.2.2 Global and volumetric efficiency

The use of the DSH introduces changes in the refrigerating plant that affects the operating conditions of the compressors. Some parameters affected by this heat exchanger are: mass flow rate, pressure ratio and temperature at the suction port.

For the LT_C, the three parameters mentioned above hardly change when the DSH is installed. Hence, the effect over the global and the volumetric efficiencies of the LT_C will be small. However, the effect of the DSH over the MT_C is higher and the suction conditions of the refrigerant and the pressure ratio are modified to a large extent. Therefore, the effect over the global and the volumetric efficiencies will be higher in the MT_C. Notwithstanding, is important to highlight that the mass flow rate will be quite similar in both configurations since the cooling capacity of the systems has been kept constants in all the tests.

Table 4 summarizes the experimental data obtained for the two compressors.

Table 4. Experimental data from the compressors.

SYSTEM	REJECTION TEMP. TEST (°C)	Compressors									
		LT_{C_POWER} (min/max) (W)	LT_{C_N} (min/max) (rpm)	$LT_{C\_T\_discharge}$ (min/max) (°C)	$LT_{C\_\eta\_GLOBAL}$ (min/max) (-)	$LT_{C\_\eta\_VOL}$ (min/max) (-)	MT_{C_POWER} (min/max) (W)	MT_{C_N} (min/max) (rpm)	$MT_{C\_T\_discharge}$ (min/max) (°C)	$MT_{C\_\eta\_GLOBAL}$ (min/max) (-)	$MT_{C\_\eta\_VOL}$ (min/max) (-)
BB	15	491 ÷ 519	948 ÷ 1006	86.3 ÷ 88.4	0.57 ÷ 0.58	0.65 ÷ 0.66	1293 ÷ 1763	1206 ÷ 1318	86.8 ÷ 114.6	0.71 ÷ 0.77	0.65 ÷ 0.74
	25	623 ÷ 684	1180 ÷ 1218	99.9 ÷ 101.0	0.54 ÷ 0.58	0.62 ÷ 0.64	1993 ÷ 2266	1559 ÷ 1633	111.2 ÷ 129.1	0.73 ÷ 0.75	0.62 ÷ 0.67
	34	651 ÷ 727	1233 ÷ 1305	100.4 ÷ 102.8	0.58 ÷ 0.61	0.65 ÷ 0.67	2945 ÷ 3092	1973 ÷ 2030	132.7 ÷ 145.4	0.74 ÷ 0.76	0.56 ÷ 0.61
BB+DSH	15	502 ÷ 523	945 ÷ 1003	85.9 ÷ 87.7	0.57 ÷ 0.59	0.64 ÷ 0.65	1259 ÷ 1718	1170 ÷ 1288	81.7 ÷ 110.1	0.76 ÷ 0.83	0.63 ÷ 0.72
	25	600 ÷ 682	1128 ÷ 1218	97.8 ÷ 100.8	0.54 ÷ 0.58	0.63 ÷ 0.64	1916 ÷ 2183	1501 ÷ 1561	105.4 ÷ 122.2	0.76 ÷ 0.81	0.6 ÷ 0.66
	34	642 ÷ 690	1206 ÷ 1341	99.4 ÷ 103.0	0.58 ÷ 0.62	0.65 ÷ 0.67	2715 ÷ 2984	1884 ÷ 1943	126.3 ÷ 139.2	0.77 ÷ 0.79	0.57 ÷ 0.6

The global and the volumetric efficiency are depicted in the Fig. 7 and Fig. 8, respectively, for both configurations as a function of the heat rejection pressure.

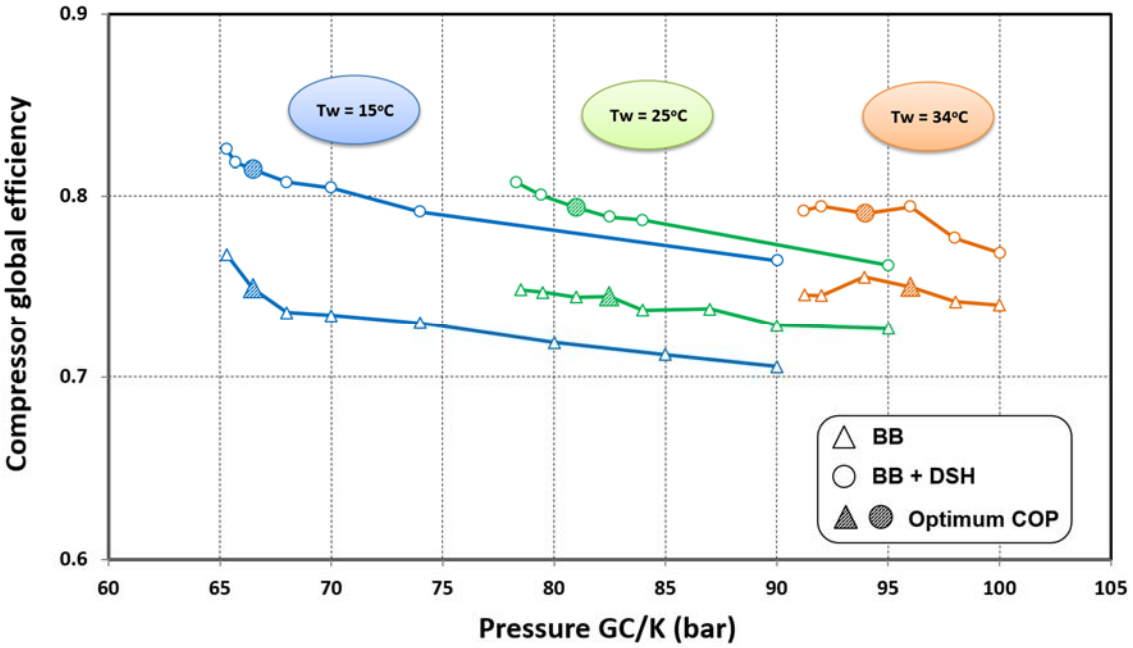

Fig. 7. MT_C global efficiency.

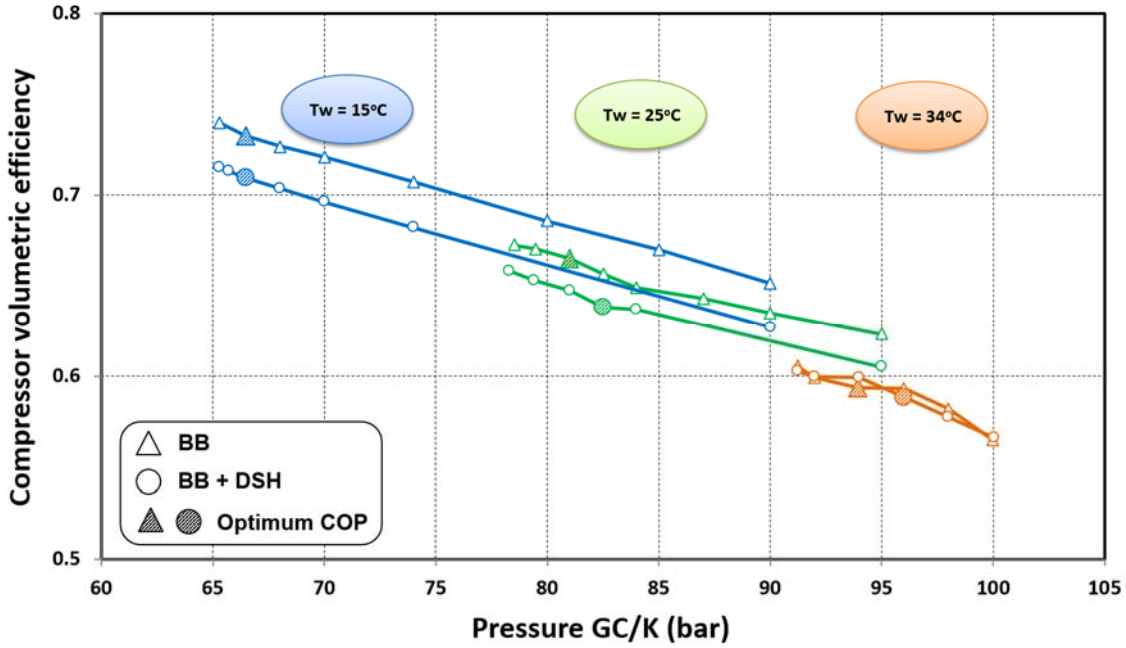

Fig. 8. MT_C volumetric efficiency.

As it shown in the Figure. 7, the global performance of the MT_C is always higher when the DSH is installed. Thus the average improvements are +8.45% at the heat rejection temperature of 15°C, +5.6% at 25°C, and +4.9% at 34°C. This is mainly due to the reduction of the specific volume at the compressor inlet port, so that for the same operating conditions, the compressor will be able to compress higher mass flow rate at same compressor velocity.

Finally, it is observed about the MT_C volumetric efficiency represented in Fig. 8 and calculated with Equation (11), that a slight reduction is produced for heat rejection temperatures of 15ºC and 25ºC when the DSH is activated. This is because the result of the multiplication of the mass flow rate variation by the suction volume variation (BB+DSH system regarding BB) is unbalanced with the variation of the compressor displacement.

Fig. 9 shows the percentage variation of the terms that affect the volumetric efficiency for the optimum operating points at each heat rejection temperature: mass flow rate ($\Delta\dot{m}_{ref}$), volume of the refrigerant at the suction port (Δv_{suc}), multiplication between these two terms ($\Delta\dot{m}_{ref} \cdot \Delta v_{suc}$) and the displacement of the compressor ($\Delta\dot{V}_G$). Additionally the volumetric efficiency ($\Delta\eta_{vol}$) is represented too.

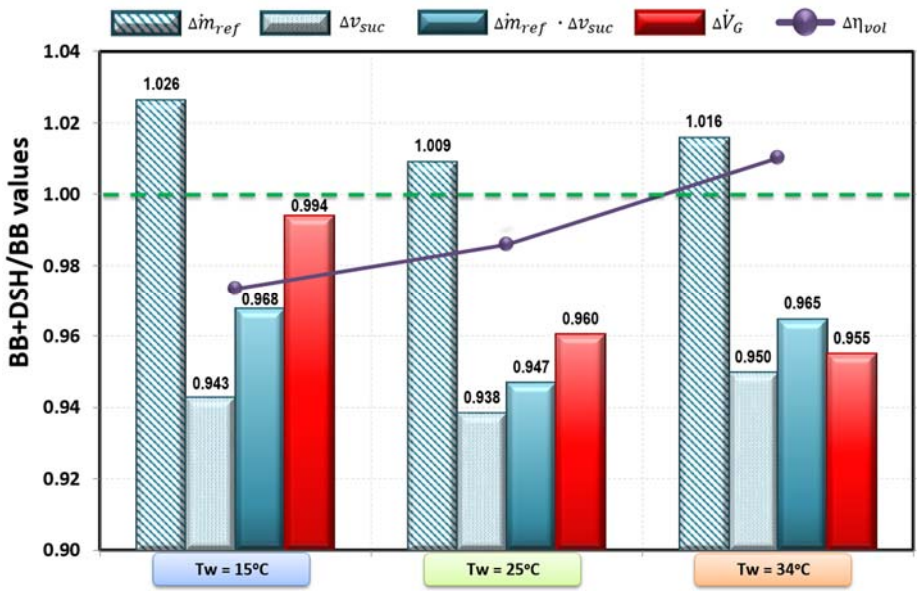

Fig. 9. Variation of values affecting the volumetric efficiency of the BB+DSH with respect to the BB.

On the one hand, the mass flow rate of the BB+DSH is slightly higher in all cases due to the GC/K optimum pressure as described in Section 5.1. On the other hand, the volume of the refrigerant at suction port and the displacement of the compressor are lower than the BB. However a greater volumetric efficiency is only achieved for heat rejection temperature of 34ºC.

5.2.3 Power consumption

Another important point in refrigeration systems is the power consumption of the compressors. In this case, DSH mainly affects to the power consumption of the medium temperature compressor (MT_C) which is shown in Fig. 10. In CO_2 Boosters, the improvements are mainly focused to reduce the power consumption of the medium temperature compressors because they have the higher contribution in the facility, what directly affects to the energy efficiency of the plant. The system with DSH reduce the consumption of the MT_C. However, this reduction is more considerably for medium-high rejection temperatures (25 and 34ºC).

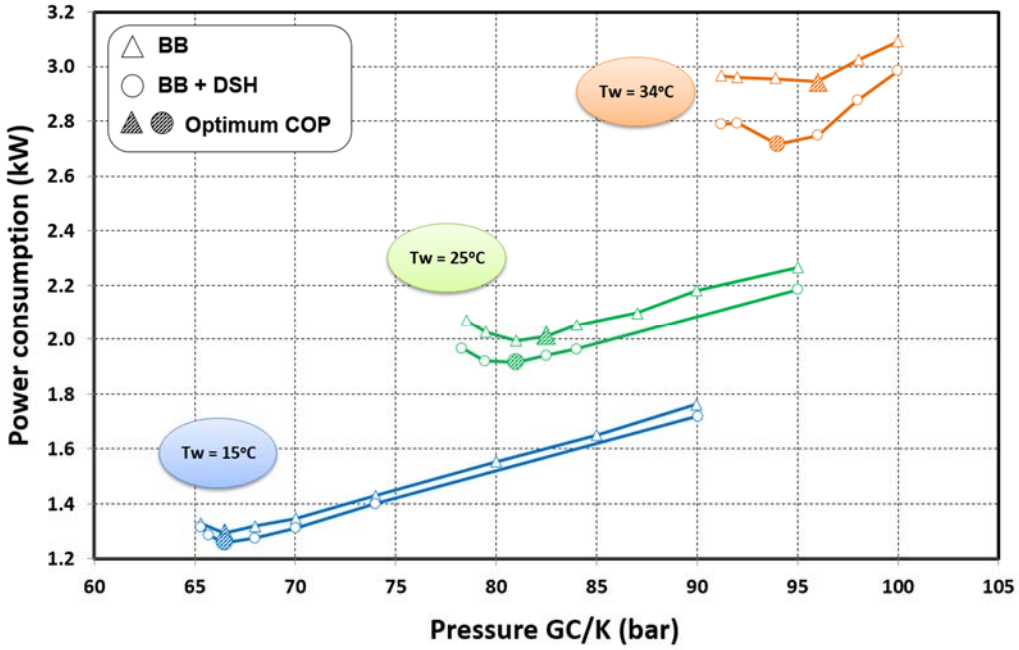

Fig. 10. MT_C power consumption.

As shown in the Table 4 , the power consumption reduction of the LT_C is insignificant at the three rejection temperatures. This is because the pressure of the receiver is quite similar working with or without DSH. For this reason, the thermophysical properties of the refrigerant at the LT_O inlet are similar too. Thus, the mass flow rate in the evaporator at the LT_C does not change for a same cooling load and neither the thermophysical properties of the refrigerant at the inlet of the LT_C.

For MT_C, the properties of the refrigerant at the compressor inlet change depending on whether the DSH is used or not. Respect to BB configuration, when DSH is connected the power reduction of the MT_C at 15ºC is only 0.62%. However, for 25ºC the power reduction is higher (4.5%) and for rejection temperature of 34ºC, a power reduction near of 8% at optimum pressure is achieved.
Again, a greater benefit is achieved as the operating conditions become worse.

5.3 COP

The last parameter to analyse is the COP of the two booster configurations analysed. In this case, the COP, depends on the power consumption of the compressors, the cooling capacities in evaporators and the power consumption of the fans as presented by Equation (1).

The power consumption of the MT_C includes the power consumption of the fan (40W) used to improve the compressor cooling. In addition, another fan of 40W ($P_{DSH,fan}$) is considered to cool the refrigerant after the LT_C as DSH. This fan is able to reject the heat needed in the DSH.

The COP evolution for BB and BB+DSH over the three rejection temperatures considered are presented in Fig. 11. As it can be observed, in all rejection temperatures analysed, the DSH provides higher COP than the basic Booster without DSH. However, the COP improvement is better for medium and high rejection temperatures.

At a rejection temperature of 15°C the optimum COP for BB and BB+DSH systems is achieved at about 66.5 bar with a maximum COP of 1.99 and 2.04 respectively. This supposes a small COP increment (up to 2.9%). However, at temperature of 25°C, the improvement at the optimum pressure increases up to 4.31%. Finally, the COP improvement for the optimum pressure at 34°C is 7.05%.

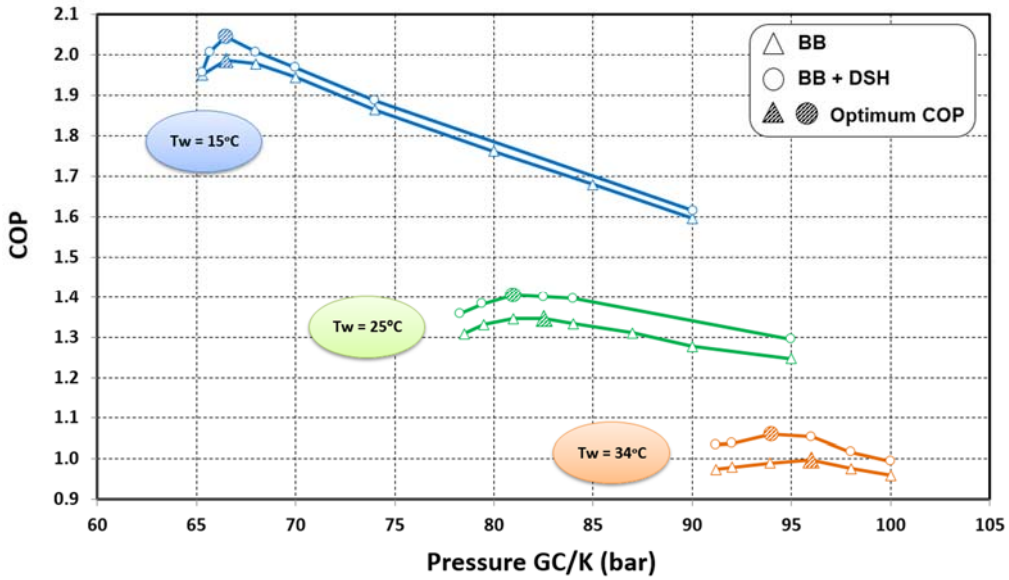

Fig. 11. COP.

6 Conclusions

This work has experimentally analysed two CO_2 Booster configurations for centralized commercial refrigeration. The two systems analysed (basic Booster and basic Booster with desuperheater) have been tested in a designed facility. These systems are evaluated for three heat rejection temperatures (15, 25 and 34°C). In addition, the evaporation levels of the two evaporators are near to -6°C at MT_O and -32°C at LT_O with a degree of superheat in the evaporators of 5K. The cooling load for LT_O (0.9 kW) and for MT_O (2.7 kW) was kept constant as well as the load ratio between the two evaporation levels (LR=3) to simulate the LR of a medium size supermarket.

The analysis covers the temperatures at the suction and discharge line of the medium temperature compressor as well the its global and volumetric efficiency, the power consumption of the compressors, the COP of each architecture for each rejection temperature and the COP improve of the BB+DSH system regarding BB.

For the evaluation of the MT_C temperature over the three rejection temperatures, it has been concluded that DSH offers a significant temperature reduction in suction and discharge line of the MT_C which is beneficial to the compressor life and to the lubricant of the MT_C.

The global efficiency of the medium temperature compressor is quite high in all cases but the introduction of the desuperheater provides improvements in global efficiencies of the MT_C from

4.9 to 8.45%. However, the volumetric efficiency with DSH for rejection temperatures of 15 and 25ºC is worse than without DSH.

For the power consumption analysis of the MT_C, DSH provides a small reduction in power (less than 1%) at rejection temperature of 15ºC, but for 25ºC, this reduction is higher than 4.5% and about 8% at rejection temperature of 34ºC.

Finally, the COP analysis shows when is more beneficial to use a DSH. Its use provides higher COP than the basic Booster without DSH in all temperatures analysed. However the COP increment is better for rejection temperatures of 25 and 34ºC. The COP improvement at 15ºC is about 2.9%, up to 4.3% at 25ºC and from 4 to 7% at 34ºC.

In conclusion, the DSH provides an improvement in COP and global efficiency of the compressors and a reduction in power consumption and suction/discharge temperatures. In addition, the temperature reduction is good for the lubricant and the MTc life. However, from an economic viewpoint, this improvement have an additional cost because it has been added a new heat exchanger in the facility and this can make it unprofitable to install a DSH due to the small increase of COP at low temperatures.

Acknowledgements

The authors gratefully acknowledge the Spanish Ministry of Economy and Competitiveness (project ENE2014-53760-R.7) (FPI BES-2015-073612) for financing this research work.

References

[1] European Parliament, Regulation (EU) No 517/2014 of the European Parliament and of the Council of 16 April 2014 on fluorinated greenhouse gases and repealing, 2014. http://eur-lex.europa.eu/legal-content/EN/TXT/PDF/?uri=CELEX:32014R0517&from=EN (accessed November 8, 2019).

[2] UNEP, The Kigali Amendment to the Montreal Protocol: HFC Phase-down, (2016). http://wedocs.unep.org/handle/20.500.11822/26589?show=full (accessed November 7, 2019).

[3] J. Catalán-Gil, D. Sánchez, R. Llopis, L. Nebot-Andrés, R. Cabello, Energy Evaluation of Multiple Stage Commercial Refrigeration Architectures Adapted to F-Gas Regulation, Energies. 11 (2018) 1915. doi:10.3390/en11071915.

[4] N. Purohit, P. Gullo, M.S. Dasgupta, Comparative Assessment of Low-GWP Based Refrigerating Plants Operating in Hot Climates, in: Energy Procedia, 2017. doi:10.1016/j.egypro.2017.03.079.

[5] R. Cabello, D. Sánchez, R. Llopis, J. Catalán-Gil, L. Nebot-Andrés, E. Torrella, Energy evaluation of R152a as drop in replacement for R134a in cascade refrigeration plants, (2017). doi:10.1016/j.applthermaleng.2016.09.010.

[6] D. Sánchez, R. Cabello, R. Llopis, J. Catalán-Gil, L. Nebot-Andrés, Á. Clemente, CO2 as secondary fluid as alternative to DX-Systems energy evaluation in a MT cabinet, in: Refrig. Sci. Technol., International Institute of Refrigeration, 2018: pp. 140–148. doi:10.18462/iir.gl.2018.1118.

[7] N. Purohit, D. Kumar Gupta, M. Sankar Dasgupta, Energetic and economic analysis of trans-critical CO2 booster system for refrigeration in warm climatic condition, Int. Jouernal Refrig. (2017).

[8] A. Cavallini, L. Cecchinato, M. Corradi, E. Fornasieri, C. Zilio, Two-stage transcritical carbon dioxide cycle optimisation: A theoretical and experimental analysis, Int. J. Refrig. 28 (2005) 1274–1283. doi:10.1016/J.IJREFRIG.2005.09.004.

[9] R. Llopis, C. Sanz-Kock, R. On Cabello, D.S. Anchez, E. Torrella, Experimental evaluation of an internal heat exchanger in a CO2 subcritical refrigeration cycle with gas-cooler, Appl. Therm. Eng. 80 (2015) 31–41. doi:10.1016/j.applthermaleng.2015.01.040.

[10] R. Cabello, D. Sánchez, J. Patiño, R. Llopis, E. Torrella, Experimental analysis of energy performance of modified single-stage CO2 transcritical vapour compression cycles based on vapour injection in the suction line, Appl. Therm. Eng. 47 (2012) 86–94. doi:10.1016/J.APPLTHERMALENG.2012.02.031.

[11] S. Elbel, P. Hrnjak, Flash gas bypass for improving the performance of transcritical R744 systems that use microchannel evaporators, Int. J. Refrig. 27 (2004) 724–735. doi:10.1016/J.IJREFRIG.2004.07.019.

[12] J. Rigola, N. Ablanque, C.D. Pérez-Segarra, A. Oliva, Numerical simulation and experimental validation of internal heat exchanger influence on CO2 trans-critical cycle performance, Int. J. Refrig. 33 (2010) 664–674. doi:10.1016/J.IJREFRIG.2009.12.030.

[13] E. Torrella, D. Sánchez, R. Llopis, R. Cabello, Energetic evaluation of an internal heat exchanger in a CO2 transcritical refrigeration plant using experimental data, Int. J. Refrig. (2010). doi:10.1016/j.ijrefrig.2010.07.006.

[14] J. Sarkar, N. Agrawal, Performance optimization of transcritical CO2 cycle with parallel compression economization, Int. J. Therm. Sci. 49 (2009) 838–843. doi:10.1016/j.ijthermalsci.2009.12.001.

[15] P. Gullo, B. Elmegaard, G. Cortella, Energy and environmental performance assessment of R744 booster supermarket refrigeration systems operating in warm climates, Int. J. Refrig. 64 (2016) 61–79. doi:10.1016/j.ijrefrig.2015.12.016.

[16] S. Minetto, R. Brignoli, C. Zilio, S. Marinetti, Experimental analysis of a new method for overfeeding multiple evaporators in refrigeration systems, Int. J. Refrig. 38 (2013) 1–9. doi:10.1016/j.ijrefrig.2013.09.044.

[17] M. Karampour, K. Samer Sawalha, K. Jaime Arias, Eco-friendly supermarkets - an overview, 2016. www.supersmart-supermarket.org (accessed October 25, 2019).

[18] J. Catalán-Gil, R. Llopis, D. Sánchez, L. Nebot-Andrés, R. Cabello, Energy analysis of dedicated and integrated mechanical subcooled CO2 boosters for supermarket applications, Int. J. Refrig. 101 (2019) 11–23. doi:10.1016/J.IJREFRIG.2019.01.034.

[19] A. Hafner, S. Försterling, K. Banasiak, Multi-ejector concept for R-744 supermarket refrigeration, Int. J. Refrig. 43 (2014) 1–13. doi:10.1016/j.ijrefrig.2013.10.015.

[20] N. Lawrence, S. Elbel, Experimental investigation on control methods and strategies for off-design operation of the transcritical R744 two-phase ejector cycle, Int. J. Refrig. (2019). doi:10.1016/j.ijrefrig.2019.04.020.

[21] C. Aprea, A. Greco, A. Maiorino, The application of a desiccant wheel to increase the energetic performances of a transcritical cycle, Energy Convers. Manag. 89 (2015) 222–230. doi:10.1016/J.ENCONMAN.2014.09.066.

[22] Bitzer, Compressors Operating Instructions KB-120-8, 2019. https://www2.bitzer.de/shared_media/documentation/kb-120-8.pdf (accessed November 9, 2019).

[23] R.J. Moffat, Using Uncertainty Analysis in the Planning of an Experiment, J. Fluids Eng. 107 (1985) 173–178. doi:10.1115/1.3242452.

[24] R. Cabello, D. Sánchez, R. Llopis, E. Torrella, Experimental evaluation of the energy efficiency of a CO2 refrigerating plant working in transcritical conditions, Appl. Therm. Eng. (2007). doi:10.1016/j.applthermaleng.2007.10.026.

[25] D. Freléchox, Field measurements and simulations of supermarkets with CO 2 refrigeration systems SE-100 44 STOCKHOLM, n.d. https://www.kth.se/polopoly_fs/1.301437.1550158491!/Menu/general/column-

content/attachment/M.Sc. Thesis-David Frelechox.pdf (accessed November 9, 2019).
[26] S. Sawalha, Theoretical evaluation of trans-critical CO2 systems in supermarket refrigeration. Part I: Modeling, simulation and optimization of two system solutions, Int. J. Refrig. 31 (2007) 516–524. doi:10.1016/j.ijrefrig.2007.05.017.
[27] S. Sawalha, Theoretical evaluation of trans-critical CO2 systems in supermarket refrigeration. Part II: System modifications and comparisons of different solutions, Int. J. Refrig. 31 (2007) 525–534. doi:10.1016/j.ijrefrig.2007.05.018.
[28] F. Kauf, Determination of the optimum high pressure for transcritical CO2-refrigeration cycles, Int. J. Therm. Sci. 38 (1999) 325–330. doi:10.1016/S1290-0729(99)80098-2.
[29] Y. Chen, J. Gu, The optimum high pressure for CO2 transcritical refrigeration systems with internal heat exchangers, Int. J. Refrig. 28 (2005) 1238–1249. doi:10.1016/J.IJREFRIG.2005.08.009.
[30] E.W. Lemmon, M.L. Huber, M.O. McLinden, NIST Standard Reference Database 23: Reference Fluid Thermodynamic and Transport Properties-REFPROP, Version 9.1, Natl Std. Ref. Data Ser. (NIST NSRDS) -. (2013). https://www.nist.gov/publications/nist-standard-reference-database-23-reference-fluid-thermodynamic-and-transport (accessed November 9, 2019).
[31] M.J. Skovrup, SecCool Properties v1.33, (2013). http://en.ipu.dk/Indhold/refrigeration-and-energy-technology/seccool.aspx.